Simulation Study of Laser-wires as a Post-Linac Diagnostic for CLIC and ILC

L. Deacon, G.A.Blair, S.P.Malton, Royal Holloway, Univ. of London, Egham, Surrey. UK.

I. Agapov, A. Latina*, D. Schulte , CERN, Geneva, Switzerland

June 20, 2008

Abstract

Realistic ILC bunch trains are simulated in the linac, including intra-train collective effects, and then analysed via a realistic simulation of a laser-wire system, including effects of laser-wire signal extraction and detection. Implications are drawn for the use of laser-wires as a post-linac machine diagnostic.

*present address: FNAL, Illinois, USA.

1 INTRODUCTION

Laser-wire (LW) systems will be used to measure transverse beam sizes at a future linear collider [1, 2] because: they can achieve micron-scale resolutions, they can withstand the power intensities in the beams, and they are essentially non-invasive devices and so can be run continuously during normal machine operation. LWs will be needed throughout the linear collider including the damping rings, ring-to-main-linac, possibly the linac itself, and the beam delivery system (BDS). R&D for such LW systems is currently ongoing [4, 5, 6].

As described in [3], the maximum number $N_{\rm det}$ of detected LW Compton events when a laser pulse collides fully-aligned with an electron bunch containing $N_e = 2 \times 10^{10}$ electrons with energy 500 GeV is approximately $N_{\rm det} \simeq 2.42 \times 10^4 \eta_{\rm det}/\sigma_m$ when a pulsed laser with peak power of 10 MW and wavelength 532 nm is used. In this expression σ_m is in μm and is given by $\sigma_m = \sqrt{\sigma_e^2 + \sigma_\ell^2}$ where σ_e is the RMS of the Gaussian electron charge distribution and σ_ℓ is the RMS laser spot size. σ_m is the convoluted size of a laser-wire scan signal in the approximation of infinite laser Rayleigh range; the full treatment for finite Rayleigh range is given in Ref [3]. $\eta_{\rm det}$ is the total detection efficiency of Compton events and is determined below by full simulations in a realistic layout for the ILC [1].

2 SIMULATION OF ILC BUNCH TRAINS

An ILC train of 2820 bunches was simulated using Placet [7]. The effects of short- and long-range wakefields in the accelerating cavities were considered, which are responsible for the most critical intra-bunch and bunch-to-bunch bunch distortions. The linac elements were misaligned using the standard RMS values foreseen for the machine after the surveyor alignment:

$\sigma_{\rm vert\ quad\ pos}$	300.0 μm
$\sigma_{\rm vert\ cavity\ pos}$	300.0 μm
$\sigma_{\rm vert\ cavity\ pitch}$	300.0 μrad
$\sigma_{\rm vert\ bpm\ pos}$	300.0 μm
BPM resolution	1 μm

then a realistic alignment procedure based on 1-to-1 correction followed by Dispersion Free Steering was applied, to minimize the emittance growth due to the misalignments. The electron bunches at the end of the linac were found to be very well described by pure Gaussian distributions with horizontal and vertical dimensions of $\sigma_x = 39.0$ μm and $\sigma_y = 1.80$ μm respectively. The main effect of the intra-train collective effects is to modulate the vertical (y) centroid positions of the Gaussian bunches as shown in Fig. 1 for the first 350 bunches.

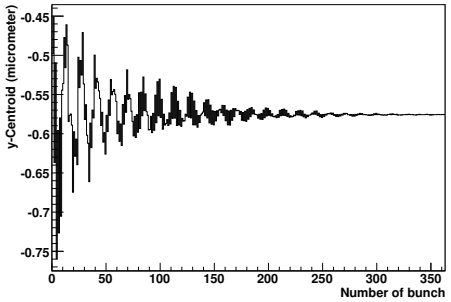

Figure 1: The vertical centroid positions of the first 350 bunches of an ILC bunch train at the exit of the linac, including wakefield effects and dispersion free steering.

This shows that, for a LW scan of a train of bunches, approximately the first 200 bunches must either be ignored, or the position of their centroids measured using fast BPMs and subtracted on a bunch-by-bunch basis [3].

3 Simulations of the ILC LW Detector Region

In the following we concentrate on a LW system located in the ILC BDS, close to the exit of the main linac as described in Ref [1]. The current ILC baseline design locates the LW detectors in the same chicane as that foreseen for the upstream polarimeter, which presents challenges for their detector location and effectiveness. In the following, full simulations are performed using the code BDSIM [8], which is based on Geant4 [9]. A detailed view of the proposed LW detector region as modelled in BDSIM, including a simulated LW Compton event, is shown in Fig. 2; it is based on a design [10] where the chicane has a fixed field with a 20 mm maximum dispersion at 250 GeV electron beam energy. The material of the vacuum chamber is stainless steel with vertical dimension 20 mm and the chamber walls are 2 mm thick and a 75 μm thick kapton window is included in front of the polarimeter detector.

4 LW Signal Detection

In principle both the electrons e_C^- and the photons γ_C from the Compton process $e^-\gamma_{\rm laser} \rightarrow e_C^-\gamma_C$ can be used to detect the LW Compton signal. In the following the various issues relating to the detection of the final state are described, together with a discussion of the main backgrounds.

4.1 Detection of γ_C

Detecting the γ_C is a challenge because it is superposed on a very large background due to synchrotron radiation (SR) from the first dipole of the chicane [11]. For this reason (discussed further below) a converter plus Cherenkov detector is proposed, with the

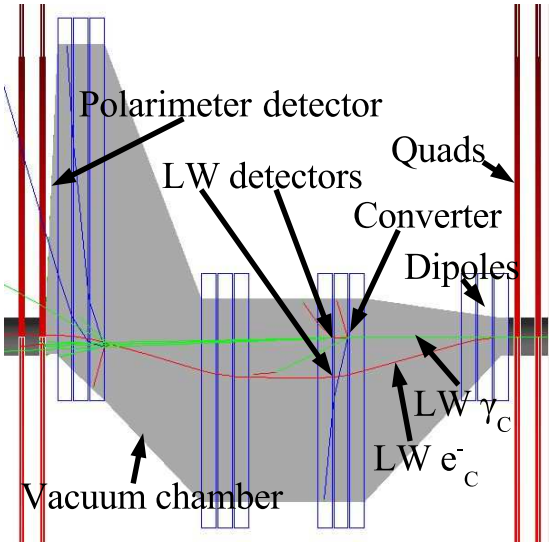

Figure 2: LW detector region/ polarimeter chicane as modelled in BDSIM. The electrons enter from the right.

Table 1: Efficiency of γ_C detection assuming a Cherenkov detector threshold of 9 MeV and a detector transverse size of 3.8 cm.

γ_C Detector Location	$\eta_{\rm det}$
After converter	0.31
After converter and dipole	0.24

detector placed downstream of one of the dipole magnets. The optimal thickness of lead converter was determined to be 3.5 mm, so as to minimise the statistical fluctuations in a downstream Cherenkov detector with threshold of 9 MeV; full details can be found in Ref. [12]. The efficiency of LW γ_C signal detection is presented in Tab. 1, where the Cherenkov detector itself is assumed to be 100% efficient for now.

4.1.1 SR Backgrounds

The SR critical energy in the first dipole of the polarimeter chicane is $E_c = 4.1$ MeV, but the γ_C energies are typically of order 10s of GeV, with a maximum energy of about 200 GeV. This difference can be exploited to separate the laser wire photon signal from the SR background by using a thin converter together with one of the chicane dipoles to form effectively a high-pass filter; one of the dipoles in the second set of triplets in the polarimeter chicane can be used naturally for this purpose. The dipole has length 2.4 m and magnetic field 0.098 T and so, if the Cherenkov detector has transverse size of about 3 cm, only tracks with energy greater than 2.8 GeV=683 E_c will be detected; the direct background from the SR photon conversions should thus be negligible.
This configuration was simulated in BDSIM using an SR generator [13] and was shown to result in negligible background from primary conversions in the converter, however

some background was found from secondary showers elsewhere in the chicane at the level of 10 tracks per bunch. This background is negligible and could be further reduced by optimising the detailed layout of the chicane.

4.1.2 Linac Backgrounds

The ILC reference design [1] locates the LW on a direct line of sight to the main linac, which means that backgrounds in this region are likely to be significant. If we assume a square converter of transverse size L, then any photon with energy greater than about 3 GeV impinging on that area would be a source of background for the γ_C detection. Any off-energy electrons are likely to be removed from the linac by over-focusing in the linac quadrupoles and so are not considered further here; however photons from the resulting electromagnetic showers may be in issue. SR from the Linac quadrupole fields has $\sim 10^2$ times lower critical energy than that from the chicane dipoles and will be subject to the same enormous reduction factors of the converter/dipole/Cherenkov system discussed above; so this potential source of background is not considered further here. This leaves beam-gas bremsstrahlung as the most likely cause of backgrounds from the linac.
The distance D of the linac relevant for producing photon background is effectively reduced by the geometric factor of the earth's curvature R_E to $D \simeq \sqrt{R_E L}$. Assuming $L = 1$ cm, this gives $D \simeq 250$ m. Being conservative and to allow for a final straight section for the linac, we now estimate the background from beam gas bremsstrahlung for $D = 300$ m. The cross-section for bremsstrahlung off N_2 or CO gas is estimated [14] to be $\sigma_B \simeq 5.51$ barns when the scattering cut-off is set at 1% of the beam energy, or in our case 2.5 GeV, which is also (conservatively) the relevant cutoff for our detection system. Assuming pressure $P = 10$ nTorr, temperature $T = 2$ K, and $N_e = 2 \times 10^{10}$ electrons per bunch, the number of background events per bunch is $DPN_e\sigma_B/k_BT$ where k_B is Boltzmann's constant, which gives about 160 bremsstrahlung photons per bunch. This is a few % of a typical peak LW signal for a vertical LW scan (the signal is 10000 γ_C for $\sigma_m \simeq 2$ μm) and about 10% for a horizontal scan (with $\sigma_m \simeq 20$ μm). While not being catastrophic for LW operation, this background level may degrade the precision of the resulting emittance measurements [3]. This is also a minimum and irreducible background; other backgrounds related to beam loss may also contribute, so clearly it would be more favourable to locate the LW after a protective bend.

4.2 Detection of e_C^-

The energies of the e_C^- are peaked at low energies due to the kinematics of Compton scattering and so they are deflected from the main beam by the dipole fields in the polarimeter chicane. A suitable Cherenkov detector could be positioned between the first and second dipole magnets in the second set of dipoles. The geometric efficiencies of e_C^- detection are shown in table 2 as a function of the clearance of the detector from the main beam, where efficiencies of order 60% are possible; this is a significant improvement on the early estimates [3].

Table 2: Efficiency of e^-_C detection as a function of the clearance distance from the edge of the detector to the main 250 GeV beam line.

Clearance [mm]	$\eta_{\rm det}$
2.5	0.95
5	0.84
7.5	0.76
10	0.68
15	0.58
20	0.50
25	0.43
30	0.38

Table 3: Number of hits in the polarimeter detector arising separately from LW and polarimeter operation, assuming 10000 Compton events per bunch for both LW and polarimeter.

From e^-_C	From γ_C	From $e^-_{C,pol}$
370 ± 60	320 ± 30	6000 ± 30

4.3 LW Background in Polarimeter Detector

The integration of LW and polarimeter within the same chicane raises the question of whether they can be operated at the same time. In order to check whether the LW signal affects the polarimeter operation, LW e^-_C and γ_C were simulated travelling through the entire length of the polarimeter vacuum chamber in the configuration described above. The number of electron and positron tracks in the polarimeter detector due respectively to LW and polarimeter operation are shown in table 3. This first study thus indicates that LW operation would generate a background of about 6% of the polarimeter signal.

5 SUMMARY

The LW detector region has been simulated in BDSIM and detection efficiencies evaluated, including effects of material interactions and secondaries. A simple calculation shows that it would be preferable to locate LW after a large bend downstream of the linac to reduce linac-related backgrounds. Preliminary simulations of wakefield effects in the linac have indicated that wakefields do not seem to affect significantly the Gaussian nature of ILC bunches, but do affect their centroid positions early in the train.

References

[1] Barish, B. and others,"ILC Reference Design Report"(2007), http://www.linearcollider.org/cms/

[2] http://clic-study.web.cern.ch/clic%2Dstudy/

[3] I. Agapov, G. A. Blair, M. Woodley " Beam emittance measurement with laser wire scanners in the International Linear Collider beam delivery system.", Phys. Rev. ST Accel. Beams 10:112801,2007.

[4] A. Bosco, and others, "A two-dimensional laser-wire scanner for electron accelerators", Nucl. Instr. and Meth. A(2008), doi:10.1016/j.nima.2008.04.012

[5] A. Aryshev, and others. These proceedings.

[6] Y. Honda,and others "Upgraded laser wire beam profile monitor", Nucl. Instrum. Meth. A538 (2005) 100-115.

[7] D. Schulte, and others, http://savannah.cern.ch/projects/placet

[8] I. Agapov, G. A. Blair, J. Carter, O. Dadoun " BDSIM: Beamline simulation toolkit based on GEANT4." EPAC'06, Edinburgh. http://www.JACoW.org.

[9] Geant4 Collaboration, Nucl. Instrum. Meth. A 506 (2003) 250-303.

[10] P. Schuler private communication, April 2008.

[11] M. Woods, K. Moffeit, "Synchrotron Backgrounds for Laserwire Detector in Upstream Polarimeter Chicane",ILC-NOTE-2008-041.

[12] L. Deacon, EUROTEV-Report-2008-18

[13] H. Burkhardt, "Monte Carlo Generation of Synchrotron Radiation", LEP-Note-632 (1990). H. Burkhardt, "Monte Carlo Generation of the Energy Spectrum of Synchrotron Radiation", EUROTEV-Report-2007-018.

[14] H. Burkhardt, L. Neukermanns, J. Resta-Lopez "Halo and Tail Generation Studies for Linear Colliders", EPAC06, Edinburgh.